

# A Tetrahedral Organophosphonate as a Linker for a Microporous Copper Framework\*\*

Jared M. Taylor, Amir H. Mahmoudkhani, and George K. H. Shimizu\*

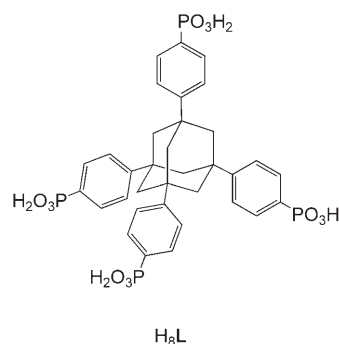
Metal–organic network solids<sup>[1]</sup> represent a compromise between wholly inorganic frameworks and wholly organic solids. While this is a self-evident statement with respect to the composition of the solids, the physical properties of the networks can also be of an intermediate nature. This type of compromise is illustrated by the thermal robustness of representative metal–organic solids and, consequently, their ability to sustain pores. Pores in any solid are typically sustained by very strong bonding to compensate for the loss in enthalpy associated with creating a void. While stability is certainly a corollary of stronger bonding, another often observed, and less desirable, consequence is a loss of long-range order. Essentially, in such cases, the growth of a network assembly from solution is sufficiently rapid that the product precipitates before an ordered assembly can be achieved, resulting in loss of crystallinity. With respect to porous solids, this rapid precipitation leads to a high dispersity of pore sizes and, hence, to non-uniform sorption properties.

Organophosphonates have been extensively studied as strongly coordinating ligands for prototypical hybrid inorganic–organic layered solids,<sup>[2]</sup> owing to their propensity to bridge a broad range of metal centers into two-dimensional sheets. With respect to porous solids, simple monophosphonate or linear diphosphonate ligands pack too efficiently to enable the formation of void space between the pillaring groups of the ligands. Smaller phosphonate or phosphate ions can be interspersed between the larger phosphonate pillars, but regular pores do not necessarily result, as the substitution is not necessarily regular.<sup>[3]</sup> More recent efforts to generate porosity have focused on using polyphosphonate ligands to disfavor the formation of simple layers<sup>[4–6]</sup> or on using template routes to form regular pores.<sup>[7]</sup> However, in general, there is an antagonistic relationship between stability and order for metal phosphonate solids: those that are robust enough to sustain pores do not typically retain high degrees of crystallinity, and, conversely, crystalline samples often do not sustain permanent pores (as shown by gas sorption).

The promise of metal–organic frameworks (MOFs) has been exemplified by recent successes in gas storage and separation by materials constructed primarily from carboxylate and pyridyl ligands.<sup>[8]</sup> With metal carboxylates, the secondary building unit (SBU) approach has been successfully employed.<sup>[9]</sup> In this methodology, an organic linker with a coordinatively divergent geometry is coupled with a well-defined metal–ligand assembly (typically a cluster) to form open frameworks by design. The metal carboxylate clusters typically targeted are those with a high tendency to form with monocarboxylate anions. Thus, these SBUs play a true structure-directing role.

With simple monophosphonate ligands, the default metal–organic structure formed is a simple layer. The extension of this motif to an open structure cannot be achieved without a major perturbation of the metal aggregates. As such, a true SBU approach does not exist for phosphonate ligands.<sup>[10]</sup>

Herein, we use a tetrahedral phosphonate ligand, 1,3,5,7-tetrakis(4-phosphonatophenyl)adamantane (**H<sub>8</sub>L**), designed



to prevent the formation of simple layers and, hence, direct the formation of an open framework upon metal complexation. The ligand **H<sub>8</sub>L** has been previously reported by us<sup>[11]</sup> and others.<sup>[5]</sup> The crystal structure of **H<sub>8</sub>L**·H<sub>2</sub>O consists of a fourfold interpenetrated diamondoid network in which the second type of tetrahedral vertex is formed by a hydrogen-bonded water–phosphonic acid cluster.<sup>[11]</sup> This result showed the predisposition of the tetrahedral ligand to form large diamondoid motifs rather than a densely packed arrangement. Very recently, complexes of **H<sub>8</sub>L** with Ti<sup>4+</sup> and V<sup>3+</sup> ions have been reported by Neumann et al.<sup>[5]</sup> No single-crystal X-ray diffraction data were reported, but the authors determined surface areas of approximately 550 and 118 m<sup>2</sup> gm<sup>−1</sup> for the titanium and vanadium solids, respectively, from N<sub>2</sub> sorption isotherms.

The crystal structure of the doubly interpenetrated diamondoid solid [Cu<sub>3</sub>(**H<sub>8</sub>L**)(OH)(H<sub>2</sub>O)<sub>3</sub>]·H<sub>2</sub>O·MeOH (**1**) is

[\*] J. M. Taylor, Dr. A. H. Mahmoudkhani, Prof. G. K. H. Shimizu  
Department of Chemistry  
University of Calgary  
Calgary, AB T2N 1N4 (Canada)  
Fax: (+1) 403-220-5347  
E-mail: gshimizu@ucalgary.ca  
Homepage: <http://www.chem.ucalgary.ca/people/academic/gshimizu/index.html>

[\*\*] This work was supported by the Department of National Defense, the Natural Sciences and Engineering Research Council (NSERC) of Canada, and the Killam Trust, through a fellowship to A.H.M. We thank Mike Benham and Kathryn Gallimore at Xonics Corporation for the sorption data.

reported herein.<sup>[12]</sup> Despite the interpenetration, a considerable open void space remains in the solid. The ligand directs the formation of trimetallic copper clusters as tetrahedral nodes, which, along with the adamantyl ligand, enable the diamondoid structure. Upon desolvation, the structure contracts to a less ordered, but structurally related phase. Notably, this desolvated material displays permanent porosity, as confirmed by CO<sub>2</sub> sorption analysis.

The ligand H<sub>8</sub>L was prepared by literature methods<sup>[5a,11]</sup> and complexed with Cu(ClO<sub>4</sub>)<sub>2</sub>·6H<sub>2</sub>O in MeOH to obtain a clear blue solution. Diffusion of hexanes into this solution resulted in the growth of small blue octahedral crystals after 2 days. Single-crystal X-ray diffraction data suggested that a monoclinic phase present in solution rapidly converts to a trigonal phase upon removal from solution. Although not immediately obvious from the unit-cell parameters (see Experimental Section for unit cell), these two solids are virtually identical with respect to their molecular structures; therefore, only the more stable trigonal phase **1** will be discussed herein.

Compound **1** has a structure based on the diamondoid net shown in Figure 1a. The formation of a diamondoid net requires a set of tetrahedral nodes, as provided by **L**, that are linked by either linear nodes or a second set of tetrahedral nodes.<sup>[13]</sup> In the case of **1**, the tricopper cluster shown in Figure 1b is the second type of tetrahedral node. Interestingly, although only three metals are involved in the cluster, the symmetry of the cluster with respect to the phosphonate ligands is tetrahedral. The three divalent copper centers form a triangular plane, which is capped on one face by a μ<sup>3</sup> phosphonate group (Cu–O21 = 1.946(3) Å), bridged on the edges by three μ<sup>2</sup> hydrogen phosphonate groups (Cu–O11 = 1.985(5) Å, Cu–O12 = 1.965(5) Å), and capped on the opposite face by a μ<sup>3</sup> hydroxo group (Cu–O1 = 2.702(7) Å). Thus, the cluster and the overall network are neutral. The coordination geometry at each copper center is square pyramidal, with the capping hydroxo group occupying the axial site. An equatorial aqua ligand completes the coordination sphere of each copper center (Cu–O1W = 2.020(10) Å).

Diamondoid nets have a topology which readily enables interpenetration to fill potential void space.<sup>[14]</sup> In **1**, twofold interpenetration is observed. Despite this interpenetration, an open channel structure is still formed, as shown in Figure 1c. Compound **1** has pore entrance widths of 4.1 Å and oval-shaped pores with a minimum width of 8.8 Å and a maximum width of 16.5 Å. Undoubtedly, the additional steric requirements of the cluster nodes prevent higher degrees of interpenetration.<sup>[15]</sup> The pores are filled by a mixture of disordered water and methanol guest molecules. Additionally, all the phenyl rings of **L** are rotationally disordered. On the basis of this promising structure, the structural integrity and porosity of the solid were examined.

The clusters in **1** are unprecedented and are interesting in that their formation can be viewed as the result of an “anti-SBU” approach. In the SBU approach, well-defined clusters and rigid spacers mutually direct the formation of a topology. As mentioned above, with phosphonate groups, no true SBUs exist as the default metal–organic structure is a simple layer. Thus, in **1**, the geometry of **L** is truly structure determining; it

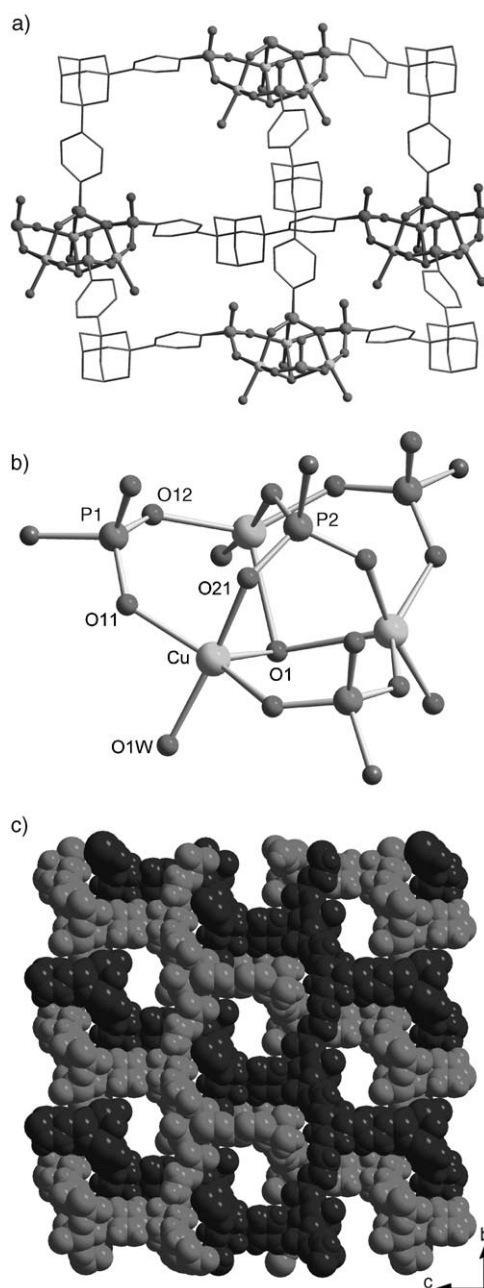


**Figure 1.** Crystal structure of **1**. a) A single diamondoid net (inorganic clusters: balls and sticks; organic linkers: wireframe). For clarity, the ligands **L** are truncated, the disordered phenyl rings are shown in the major orientation, and the H atoms are omitted. b) A cluster node comprising three Cu<sup>2+</sup> centers, one OH<sup>−</sup> ion (O1), three H<sub>2</sub>O molecules (O1W), and tetrahedrally oriented RPO<sub>3</sub>H<sup>−</sup> (P1) and RPO<sub>3</sub><sup>2−</sup> (P2) groups. For clarity, the H atoms are omitted. c) A space-filling representation of the doubly interpenetrated diamondoid network.

directs not only the overall diamondoid topology, but also the geometry of the resultant metal cluster. This is a key point in that new metal aggregates must result in a diamondoid network complex of **L**.

Thermogravimetric analysis (TGA) showed a loss of solvent in three steps (from room temperature to 155 °C, 10.1%; from 155–235 °C, 7.7%; from 235–275 °C, 5.8%),

followed by a plateau (from 275–405 °C). An exothermic peak in the differential scanning calorimetry (DSC) trace accompanied the second mass loss. Upon heating the initial monoclinic solid, variable-temperature powder X-ray diffraction (PXRD) revealed the emergence of a new peak at  $2\theta = 6.6^\circ$  (Figure 2). The PXRD experiment also indicated a loss of long-range order in the solid: there is a gradual loss of peak intensity from room temperature to 280 °C by DSC. Heating to 230 °C is shown in Figure 2, but the broadened peaks at

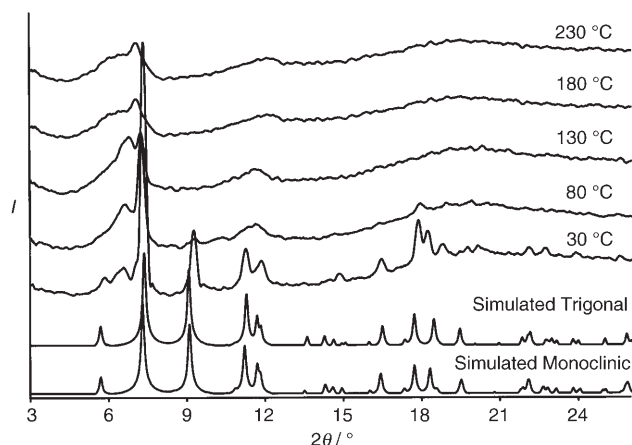


**Figure 2.** PXRD patterns for **1** on heating from 30–230 °C, as well as simulated patterns for the trigonal and monoclinic phases.

high temperatures still correspond to the original phase (the broadening can also be partly attributed to the increased thermal motion of the atoms at the higher temperature of the analysis). These results indicate an increased distortion of the network without a complete collapse.

To confirm that pores exist within the network, CO<sub>2</sub> sorption analyses were performed on a sample heated at 120 °C for 20 h (not shown). A type-I isotherm, characteristic of a microporous solid, was observed. Dubinin–Radushkevich line fitting gave a surface area of 198 m<sup>2</sup> gm<sup>−1</sup> and an average pore width of 5.0 Å. These values are comparable to those for smaller-pore zeolites and, importantly, confirm that there are accessible micropores in **1**. The desorption cycle showed evidence of hysteresis, which could indicate an activation of the solid by CO<sub>2</sub>. Given that the copper cluster in **1** contains a bridging hydroxide ion and three hydrogen phosphonate groups, a plausible pathway for the structural distortion could involve the elimination of water. A fluoride–hydroxide ion exchange was conducted by suspending **1** in a solution of (Bu)<sub>4</sub>NF in hexanes for 2 weeks. The DSC trace of the resulting solid did not possess the marked exothermic peak associated with the second mass loss of **1**, but the PXRD patterns of the solid suggested a similar structural distortion with increasing temperature. When a control experiment was carried out by suspending **1** in hexanes alone, the exothermic transition was still detected by DSC for the resulting solid. For the fluoride-exchanged solid, a surface area of 182 m<sup>2</sup> gm<sup>−1</sup> was determined from the CO<sub>2</sub> sorption isotherm; however, no hysteresis was observed, even in a second complete sorption cycle (Figure 3). This observation confirmed that structure is

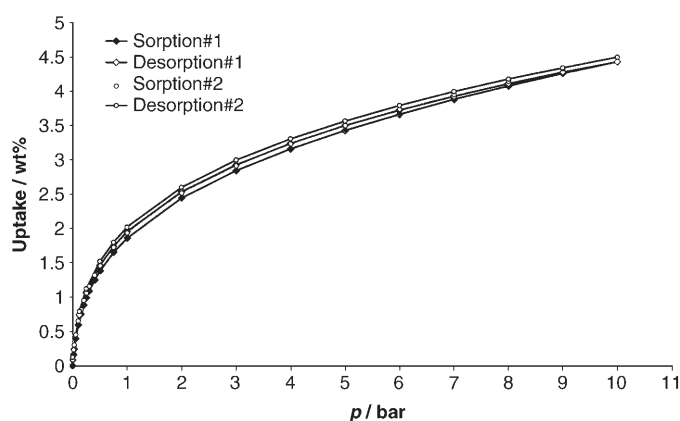


**Figure 3.** Two cycles of CO<sub>2</sub> adsorption/desorption for a fluoride-exchanged sample of **1** conducted at 0 °C.

rigid and is not activated by CO<sub>2</sub>. Considering this result together with the PXRD data, it is unlikely that the exchanged solid has a significantly different structure; the fluoride exchange does, however, rigidify the porous structure.

As metal clusters and metal–oxygen bonds have been cited as the primary sites for H<sub>2</sub> adsorption in MOFs, an approach coupling porosity with new metal–oxo clusters could potentially lead to improved H<sub>2</sub> storage materials. In the case of **1**, the H<sub>2</sub> storage capacity was measured to be 0.24 wt %, which is not a high value.

A second intriguing possibility is the potential for magnetic exchange interactions within and/or between the clusters, which could lead to porous magnetic solids. Preliminary magnetic measurements on **1** indicate that antiferromagnetic exchange interactions between the copper centers occur within the clusters. A more complete study of the magnetic and O<sub>2</sub> sorption properties of **1** will follow. Very recently, two networks with hydroxo-bridged tricopper clusters and bridging triazolate ligands have been reported.<sup>[16]</sup> The clusters in these networks also exhibit antiferromagnetic exchange interactions.

We have presented a microporous phosphonate network containing unprecedented metal clusters. These clusters are a direct result of the structure-directing role of the ligand. This “anti-SBU” approach necessitates the formation of novel metal aggregates if a stable network is to result. As phosphonate ligand cores with different geometries would require different metal aggregates to form, this approach offers a route to a diverse array of porous compounds, as well as to networks incorporating new inorganic motifs, which could be associated with interesting physical properties.

## Experimental Section

Ligand **L** was prepared as the tetraphosphonic acid H<sub>8</sub>**L** according to the published procedure.<sup>[5a,11]</sup> H<sub>8</sub>**L** (0.053 mmol) was dissolved in MeOH (3 mL) and mixed with Cu(ClO<sub>4</sub>)<sub>2</sub>·6H<sub>2</sub>O (0.219 mmol) dissolved in MeOH (3 mL) to obtain a clear blue solution. The mixture was then placed in a vial, and the vial was placed over hexanes (20 mL) in a sealed jar to allow the slow diffusion of hexanes

into the mixture. Small blue hexagonal crystals grew after 2 days. IR:  $\tilde{\nu}$  = 3498 (w), 1604 (s), 1397 (s), 1151 (w), 704 (s), 567 (m). Single-crystal X-ray diffraction data indicate that **1** crystallizes as a monoclinic phase  $P2_1/n$  (No. 14)  $a = 15.899(3)$ ,  $b = 18.788(4)$ ,  $c = 24.719(5)$  Å,  $\beta = 104.92(3)^\circ$  in solution, which transforms to a trigonal phase upon removal from solution. Owing to the number of volatile components, elemental analyses were not performed on the crystals.

Received: September 30, 2006

Published online: December 13, 2006

**Keywords:** cluster compounds · copper · metal–organic frameworks · microporous materials · phosphonates

- [1] a) S. Kitagawa, R. Kitaura, S. Noro, *Angew. Chem.* **2004**, *116*, 2388; *Angew. Chem. Int. Ed.* **2004**, *43*, 2334; b) M. Eddaoudi, J. Kim, N. Rosi, D. Vodak, J. Wachter, M. O’Keeffe, O. M. Yaghi, *Science* **2002**, *295*, 469; c) J. L. C. Rowsell, O. M. Yaghi, *Microporous Mesoporous Mater.* **2004**, *73*, 3.
- [2] a) A. Clearfield, *Prog. Inorg. Chem.* **1998**, *47*, 371; b) G. Alberti, U. Costantino in *Comprehensive Supramolecular Chemistry*, Vol. 7 (Eds.: J. L. Atwood, J. E. D. Davies, D. D. MacNicol, F. Vögtle), Elsevier Science, New York, **1996**; c) K. Maeda, *Microporous Mesoporous Mater.* **2004**, *73*, 47.
- [3] a) G. Alberti, U. Costantino, F. Marmottini, R. Vivani, P. Zappelli, *Angew. Chem.* **1993**, *105*, 1396; *Angew. Chem. Int. Ed. Engl.* **1993**, *32*, 1357; b) G. Alberti, F. Marmottini, S. Murcia-Mascarós, R. Vivani, *Angew. Chem.* **1994**, *106*, 1655; *Angew. Chem. Int. Ed. Engl.* **1994**, *33*, 1594; c) N. J. Clayden, *J. Chem. Soc. Dalton Trans.* **1987**, 1877; d) M. D. M. Gómez-Alcántara, A. Cabeza, L. Moreno-Real, M. A. G. Aranda, A. Clearfield, *Microporous Mesoporous Mater.* **2006**, *88*, 293.
- [4] a) O. R. Evans, D. R. Manke, W. Lin, *Chem. Mater.* **2002**, *14*, 3866; b) O. R. Evans, H. L. Ngo, W. Lin, *J. Am. Chem. Soc.* **2001**, *123*, 10395; c) H. L. Ngo, W. Lin, *J. Am. Chem. Soc.* **2002**, *124*, 14298.
- [5] a) M. V. Vasylyev, E. J. Wachtel, R. Popovitz-Biro, R. Neumann, *Chem. Eur. J.* **2006**, *12*, 3507; b) M. Vasylyev, R. Neumann, *Chem. Mater.* **2006**, *18*, 2781.
- [6] a) D. Kong, J. Zon, J. McBee, A. Clearfield, *Inorg. Chem.* **2006**, *45*, 977; b) N. Stock, N. Guillou, J. Senker, G. Férey, T. Bein, Z. Anorg. Allg. Chem. **2005**, *631*, 575; c) J. A. Groves, N. F. Stephens, P. A. Wright, P. Lightfoot, *Solid State Sci.* **2006**, *8*, 397.
- [7] G. B. Hix, A. Turner, B. M. Kariuki, M. Tremayne, E. J. MacLean, *J. Mater. Chem.* **2002**, *12*, 3220.
- [8] a) X. Zhao, B. Xiao, A. J. Fletcher, K. M. Thomas, D. Bradshaw, M. J. Rosseinsky, *Science* **2004**, *306*, 1012; b) R. Matsuda, R. Kitaura, S. Kitagawa, Y. Kubota, R. V. Belosludov, T. C. Kobayashi, H. Sakamoto, T. Chiba, M. Takata, Y. Kawazoe, Y. Mita, *Nature* **2005**, *436*, 238; c) M. Eddaoudi, J. Kim, N. Rosi, D. Vodak, J. Wachter, M. O’Keeffe, O. M. Yaghi, *Science* **2002**, *295*, 469; d) B. L. Chen, C. Liang, J. Yang, D. S. Contreras, Y. L. Clancy, E. B. Lobkovsky, O. M. Yaghi, S. Dai, *Angew. Chem.* **2006**, *118*, 1418; *Angew. Chem. Int. Ed.* **2006**, *45*, 1390; e) M. Eddaoudi, H. Li, O. M. Yaghi, *J. Am. Chem. Soc.* **2000**, *122*, 1391; f) D. N. Dybtsev, H. Chun, S. H. Yoon, D. Kim, K. Kim, *J. Am. Chem. Soc.* **2004**, *126*, 32; g) L. Pan, M. B. Sander, X. Huang, J. Li, M. Smith, E. Bittner, B. Bockrath, J. K. Johnson, *J. Am. Chem. Soc.* **2004**, *126*, 1309.
- [9] J. Kim, B. Chen, T. M. Reineke, H. L. Li, M. Eddaoudi, D. B. Moler, O’Keeffe, O. M. Yaghi, *J. Am. Chem. Soc.* **2001**, *123*, 8239.
- [10] A few examples of metal phosphonate clusters exist, but their structural regularity does not merit the SBU designator: a) M. I. Khan, J. Zubieta, *Prog. Inorg. Chem.* **1995**, *43*, 1; b) Y. Yang, J. Pinkas, M. Noltemeyer, H.-G. Schmidt, H. W. Roesky, *Angew. Chem.* **1999**, *111*, 706; *Angew. Chem. Int. Ed.* **1999**, *38*, 664; c) W. F. Ruettinger, D. M. Ho, G. C. Dismukes, *Inorg. Chem.* **1999**, *38*, 1036; d) E. Dumas, C. Sassoey, K. D. Smith, S. C. Sevon, *Inorg. Chem.* **2002**, *41*, 4029; e) C. Lei, J.-G. Mao, Y.-Q. Sun, H.-Y. Zeng, A. Clearfield, *Inorg. Chem.* **2003**, *42*, 6157; f) V. Chandrasekhar, S. Kingsley, *Angew. Chem.* **2000**, *112*, 2410; *Angew. Chem. Int. Ed.* **2000**, *39*, 2320; g) E. K. Brechin, R. A. Coxall, A. Parkin, S. Parsons, P. A. Tasker, R. E. P. Winpenny, *Angew. Chem.* **2001**, *113*, 2772; *Angew. Chem. Int. Ed.* **2001**, *40*, 2700; h) V. Chandrasekhar, P. Sasikumar, R. Boomishankar, G. Anantharaman, *Inorg. Chem.* **2006**, *45*, 3344.
- [11] K. M. E. Jones, A. H. Mahmoudkhani, B. D. Chandler, G. K. H. Shimizu, *CrystEngComm* **2006**, *8*, 303.
- [12] Crystal data for  $[\text{Cu}_3(\text{H}_3\text{L})(\text{OH})(\text{H}_2\text{O})_3] \cdot \text{H}_2\text{O} \cdot \text{MeOH}$  (**1**):  $M_r = 1017.14$ ,  $\text{C}_{35}\text{H}_{44}\text{Cu}_3\text{O}_{18}\text{P}_4$ , trigonal, space group  $R\bar{3}$  (no. 148),  $a = 18.812(3)$ ,  $c = 34.892(7)$  Å,  $V = 10694(3)$  Å<sup>3</sup>,  $Z = 6$ ,  $\rho_{\text{calc}} = 0.948 \text{ Mg m}^{-3}$ ,  $\mu(\text{Mo K}\alpha) = 1.016 \text{ mm}^{-1}$ , crystal size  $0.46 \times 0.34 \times 0.32 \text{ mm}^3$ . Data were collected on a Nonius KappaCCD diffractometer using  $\text{Mo K}\alpha$  radiation. A total of 28465 reflections ( $1.75 < \theta < 25.42^\circ$ ) were processed, of which 3347 were considered unique and significant (with  $I > 2\sigma(I)$ ). Structure solution and refinement, and graphics preparation were carried out with the SHELX97 software package (release 5.1).<sup>[17]</sup> For  $I > 2\sigma(I)$ ,  $R1 = 0.1480$ ,  $wR2 = 0.3690$ ,  $\text{GoF} = 1.519$ , 214 parameters, 21 restraints. CCDC-622574 contains the supplementary crystallographic data for this paper. These data can be obtained free of charge from The Cambridge Crystallographic Data Centre via [www.ccdc.cam.ac.uk/data\\_request/cif](http://www.ccdc.cam.ac.uk/data_request/cif).
- [13] M. J. Zaworotko, *Chem. Soc. Rev.* **1994**, *23*, 283.
- [14] N. L. Rosi, M. Eddaoudi, J. Kim, M. O’Keeffe, O. M. Yaghi, *CrystEngComm* **2002**, *2*, 401.
- [15] B. L. Chen, M. Eddaoudi, S. T. Hyde, M. O’Keeffe, O. M. Yaghi, *Science* **2002**, *295*, 469.
- [16] W. Ouellette, M. H. Yu, C. J. O’Connor, D. Hargman, J. Zubieta, *Angew. Chem.* **2006**, *118*, 3577; *Angew. Chem. Int. Ed.* **2006**, *45*, 3497.
- [17] G. M. Sheldrick, SHELX97, Program for Crystal Structure Refinement, University of Göttingen, Göttingen (Germany), **1997**.